

COMPARATIVE STUDY OF COASTLINE CHANGES USING THE IJIMA SATO SEDIMENT TRANSPORT METHOD IN RELATION TO THE CONSTRUCTION OF GROIN STRUCTURES IN THE RANDUPUTIH BEACH AREA, PROBOLINGGO REGENCY

Yani Nurita Purnawanti^{1*}, Muh. Kasim², Debrina Alfitri Kentania³, Hasan Ikhwan⁴

Submitted: June 27, 2024 Accepted: July 22, 2024.

¹Department of Fishery Mechanization, Marine and Fisheries Polytechnics, Sorong

²Department of Fishing Technique, Marine and Fisheries Polytechnics, Sorong

³Department of Ocean Engineering, Faculty of Marine Technology, Sepuluh Nopember Institute of Technology

Corresponding author:

*Yani Nurita Purnawanti

Email: nurita@polikpsorong.ac.id

ABSTRACT

As the population increased, the requirement for housing increased as well. The Randuputih coastal area on the coasts of Probolinggo Regency is located in the northern part of Java Island, so most residential areas are in the north coastal area. In this area, there is housing development close to the coastal area. With the housing development near the Probolinggo coastal area, we plan to build a coastal protection building as a groin structure to prevent erosion along the coast. In designing the groin structure, it is necessary to analyze the coastline changes in the Randuputih coastal area, Probolinggo Regency, to calculate the length of the groin built in that area. As a reference for calculating the groin structure, the analysis carried out observed changes in the coastline over 20 years (2003-2023). The sediment transport method used is the Ijima Sato sediment transport method because this method approximates changes in coastlines based on observations over 20 years in the Randuputih coastal area, Probolinggo Regency. The average sediment transport is 3.74 m³/day from the northwest. Adding three groin structures along 700m can maintain coastline change stability by up to 6.61%. Before the groins were applied, the average coastline change was 34%.

Keywords: Sediment transport, Groins, Coastline Changes, Erosion, Randuputih

INTRODUCTION

The beach is the boundary between land and sea, where every year, the coastline experiences changes, both in terms of erosion and sedimentation. One of the causes of changes in the coastline every year is fluctuations in sea level, tides, sediment transport, and coastal sediment transport or nearshore sediment transport (Triatmodjo, 1999). Coastal sediment transport is sediment movement in coastal areas caused by waves and the currents they generate. In the area where the wave breaks, usually called the surf zone, there is a confluence of sediment movements towards the beach and those moving back towards the middle of the sea. In addition, sediment movement outside the surf zone will begin to weaken. Longshore currents will move sediment material near the coast (Hanes, 2022). This results in longshore sediment transport (longshore drift).

The phenomenon of wave direction changing due to depth-induced variations in phase velocity in the lateral direction (i.e., along the wave crest) is called refraction. It turns out that the wave direction is towards shallow water and results in an increase or decrease in wave height, depending on the actual change of wave direction (Marghany, 2021). This affects longshore sediment transport rates along the

coast, as shown in the study by (Fellowes et al., 2021) on beaches in estuaries and bays (BEBs).

The sedimentation process involves depositing sediment grains from water pools to the bottom of the waters. In waters, this process includes release in suspended form suspension, saltation, rolling, and sliding. Furthermore, these granules will settle if the water flow cannot maintain its movement. In coastal areas characterized by fine sand sediments, the sedimentation process is influenced by oceanographic activity in the form of currents, waves, and tides. (Purba et al., 2022). The problem in the Randuputih coastal area of Probolinggo Regency is erosion that occurs around residential areas. This area has housing development close to the coastal area, with housing development near the Probolinggo coastal area, so groin-type coastal protection buildings will be applied. The construction of groins can also cause changes in the coastline. This is related to recent studies on coastline changes at Icaraf Beach, Northeast Brazil (Gurgel Vasconcelos et al., 2024) and along the coast of Ghana (Donatus et al., 2023). Therefore, conducting more in-depth calculations and analyses using comprehensive methods and erosion management strategies is necessary to predict potential future erosion due to coastal protection structures (Manno et al., 2022).

The results of the analysis show that the downstream side of the groin experienced abrasion and the upstream side of the groin experienced accretion, which is influenced by several factors such as the amount of abrasion and accretion, the direction of the angle of incidence of the wave, the amplitude of sediment transport along the coast, the depth of the water when the wave breaks, and the angle of incidence of the breaking wave (Paul et al., 2022). Permeable groins can control sediment transport along the coast without causing erosion in the downdrift groin so that changes in the coastline between updraft groins and downdrift groins are not too extreme (Umar et al., 2023).

Several studies use the sediment transport calculation method, namely the Rotner van Rijin method (Pratama et al., 2019). The Shen and Hung Method and the Engelund and Hansen Method, which have the least sediment transport results (Kumaseh et al., 2020). The Manohar, Komar, and CERC method considers wave factors, initial coastline, sediment characteristics, and seabed slope in calculating coastline changes due to longshore sediment transport (Fernandes & Castro, 2024). Calculations using the CERC method are widely used in studies of coastal topologies, such as those on the Brazilian coast. (Carvalho & Guerra, 2024) (Trombetta, 2020).

As previously known, the movement of coastal sediment may be caused by river currents, waves, tidal currents, wind, and sand mining around the coast. Sediment originating from erosion of rivers, coastal cliffs, and seabeds is likely to be transported offshore by rip currents. Increased sedimentation in areas that initially experienced erosion. Through this study, a model of coastline changes due to erosion and sedimentation was studied before and after the groin building concerning sediment transport using the Ijima Sato method.

MATERIALS AND METHODS

Changing the coastline can occur due to someone moving from one place to another, and this causes soil erosion from a particular place. Therefore, erosion occurs in one place and sedimentation in another.

Coastline changes include erosion and acceleration. In this case, it is also influenced by sediment transport, a natural phenomenon often found in coastal engineering. This sediment transport is essential in planning a coastal protection structure building to know the changes in the coastline.

Data Collection

This research was conducted in the coastal area of Randuputih village, Probolinggo Regency, which is

1.5 kilometers long. The data used includes wind and tidal data obtained from BMKG Surabaya in 2021-2022 and bathymetric maps of the Probolinggo area. Bathymetry map in 2003 and Google Earth map in 2023.

Calculation of Coastline Changes

The analysis of Coastline Change explains the process of changes in the profile and coastline, using analysis methods obtained from sediment transport calculations, a prediction calculation of changes in the shoreline for five years and at the same time for 20 years can be obtained so that the coastline model after the next 20 years can describe the profile of changes in the coastline. Several formulas are used to calculate sediment transport. The calculations we have carried out using the Ijima Sato sediment transport method are used because, in the analysis of changes in coastlines, it is closest to changes in coastlines over 20 years in the Randuputih area, Probolinggo Regency.

The first process of calculation using sediment transport is wind data. Wind data obtained from BMKG (Meteorology, Climatology, and Geophysics Council) Surabaya was processed with the help of WRPlot software to determine the dominant wind direction in the Probolinggo area. The wind data inputted is speed and direction taken every hour via the BMKG satellite. Figure 1 shows that the dominant wind is from the northwest at 40% with a maximum speed of 6-8 knots, but at most, it has a speed of 2-4 knots. So, we get the dominant wind direction from the northwest in the northern coastal observation area of Probolinggo Regency.

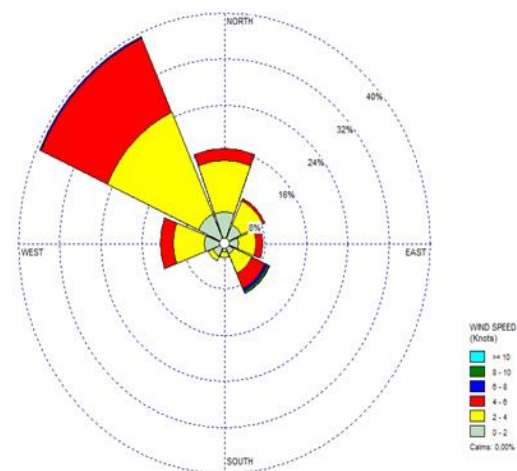


Figure 1. Windrose

Then, the fetch in Figure 2, the area of wind gusts that can generate waves, is determined by plotting a map and drawing a line that shows the dominant wind direction on the map, where the dominant

wind direction refers to the WRPlot windrose results.

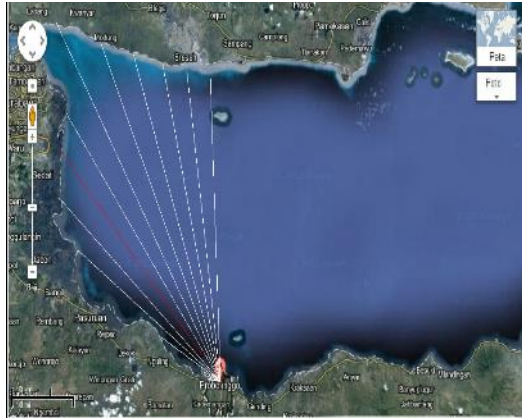


Figure 2. Fetch in the northwest direction or direction 135^o

$$F_{eff} = \frac{\sum Xi \cos \alpha_i}{\sum \cos \alpha_i}$$

Where :

Feff: effective fetch

Xi: fetch line length

α_i : deviation on both sides from the wind direction, using increments of 6° to an angle of 42° on both sides of the wind direction.

Effective Fetch Calculation Results,

Feff = 242.456,87 m

Usually, wind measurements are made on land, even though the wind data is used on the sea surface in wave generator formulas. Therefore, it is necessary to transform wind data over land (UL) closest to the study location to wind data over sea level (UW). By reading the graph in Figure 3, the UW value is obtained for each input wind speed. The results are shown in Table 1.

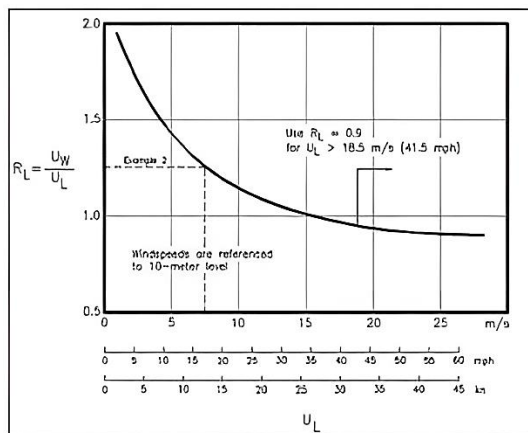


Figure 3. Wind to Wave Conversion Graph

Where;

U A: wind stress factor

U L: wind speed over land (m/s)

U W: wind speed above sea level (m/s)

R L: relationship U L and U W (wind speed on land and sea)

Table 1. Wind Stress Factor (UA)

No.	U _L		R _L	U _W	U _A
	knots	m/s		m / s	
1	0	0.00	0.000	0.00	0.00
2	2	1.03	1.850	1.90	1.57
3	4	2.06	1.650	3.40	3.19
4	6	3.09	1.500	4.63	4.68
5	8	4.12	1.400	5.76	6.12
6	10	5.14	1.325	6.82	7.53
7	12	6.17	1.275	7.87	8.98
8	14	7.2	1.225	8.82	10.34
9	16	8.23	1.150	9.47	11.27

After obtaining the U_w value from reading the graph in Figure 3, calculate the UA value using the equation below. The results of the UA calculation for each wind speed can be seen in Table 1.

$$U A = 0.71 \times U W^{1.23}$$

$$R L = U W / U L$$

$$Hm0 = 5.112 \times 10^{-4} \times U A \times F^{0.5}$$

$$Tm = 6.238 \times 10^{-2} \times [U A \times F]^{0.33}$$

Hrms: H root mean square (m)/centering average height

$$Hs = 1.416 \times Hrms$$

Hs: significant wave height (m)

Havg: average deep sea wave height (m)

Tavg: average deep sea wave period (s)

$$Hrms = 0.92 \text{ m}$$

$$Trms = 5.62 \text{ s}$$

$$H(1/3) = 1.31 \text{ m}$$

$$T(1/3) = 7.96 \text{ s}$$

$$Tavg = 5.01 \text{ s}$$

$$Havg = 0.97 \text{ m}$$

The probability is determined for each wave height as follows: Fisher-Tippett Type I Distribution (k=0.75)

$$P(Hs \leq \hat{H}sm) = 1 - \frac{m-0.44}{N_r+0.12}$$

Where:

P(Hs ≤ $\hat{H}sm$): probability of the mth representative wave not being exceeded

$\hat{H}sm$: m-th order wave height

m: significant wave height sequence number 1,2,3..N

N T: Number of wave events during recording (can be greater than the representative wave)

$$H_m = A y_m + B$$

Where:

y_m is given by the following form, for the Fisher-Tippet type I distribution $y_m = -\ln \{-\ln F(H_s - H_{sm})\}$,
 $H_{sr} = \hat{A} Y_r + B$

Where:

Y_r is given by the following form, $Y_r = \{\ln(LT_r)\}^{1/k}$
 H_{sr} : Significant wave height with return period T_r
 T_r : Return period (years)
 K : length of data (years)
 L : average number of events per year $= N T / k$

Wave Refraction (Figure 4) is the event of a change in the direction of wave crest motion. Wave refraction and shallowing (wave shoaling) will determine the wave height in a place based on the characteristics of the incoming wave. Refraction has a significant influence on wave height and direction, as well as the distribution of wave energy along the coast.

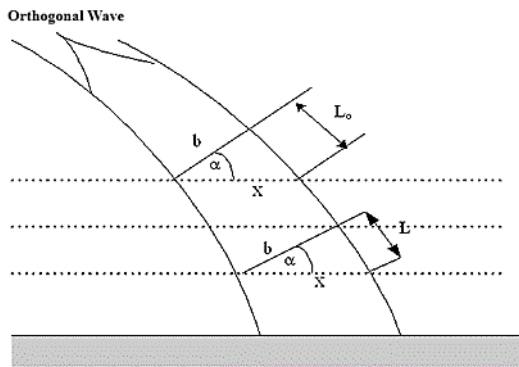


Figure 4. Wave Refraction on Straight and Parallel Contours

$$\sin \alpha = \left(\frac{C}{C_0}\right) \sin \alpha_0$$

Where:

α_0 : The angle between the wave crest and the basic contour
 α : The same angle measured when the wave crest line crosses the bottom contour
 C_0 : Wave speed at the first contour
 C : Wave speed at the second contour

Wave transformation analysis is often carried out using equivalent deep sea waves, namely the height of waves in the deep sea if they do not experience refraction. The equivalent deep sea wave height is given in the equation. (Triatmodjo, 1999):

$$L_0 = 1.56 \times T^2$$

$$C_0 = L_0 \times T$$

$$C = L \times T$$

$$\sin \alpha = (C/C_0) \times \sin \alpha_0$$

$$K_r = (\cos \alpha_0 / \cos \alpha)^{0.5}$$

$$K_s = (n_0 \times L_0 / n \times L)^{0.5}$$

$$H'_o = K_s \times K_r \times H_o$$

Where :

H'_o : equivalent deep sea wave height
 H_o : height of deep-sea waves
 L_o : height of deep-sea waves
 K_s : diffraction coefficient
 K_r : coefficient of refraction

Breaking waves are influenced by their slope, namely the ratio between height (H) and wavelength (L). In the deep sea, the maximum wave slope at which the wave begins to become unstable is given by the following form;

$$\frac{H}{L} = \frac{1}{7} \quad \frac{H_o}{H'_o} = \frac{1}{3.3(H'_o/L_o)^{1/3}}$$

$$\frac{db}{Hb} = 1,28 \quad \frac{db}{Hb} = \frac{1}{b - (aHb/gT^2)}$$

$$a = 43,75(1 - e^{-19m}) \quad b = \frac{1,56}{(1 + e^{-19.5m})}$$

Where :

Db : Depth of breaking wave
 Hb : Height of breaking wave

The existing formula for calculating sediment transport along the coast was developed based on model and prototype measurement data on sandy beaches. Some of these formulas below are simple relationships between sediment transport and longshore components in the form:

$$Q_s = K P_1^n \quad P_1 = \frac{\rho g}{8} H_b^3 \sin \alpha_b \cos \alpha_b$$

Where:

Q_s : Sediment transport along the coast (m^3/day)
 P_1 : Wave energy flux component along the coast at the time of breaking ($Nm/d/m$)
 H_b : Height of the breaking wave
 α_b : Angle of incidence of the breaking wave
 K, n : Constant

This article uses the Ijima Sato ($Q_s = 0.060 \times P_1$) sediment transport calculation method, which will be validated with other methods. Sediment transport formulas (Table 2), contained in the coastal engineering book (Bambang Triatmodjo, 1999).

Validation

In this case, initial data is obtained that can support the existence of a sedimentation process, including erosion, transportation, and deposition. This process is very complex, starting from the fall of rain, which produces kinetic energy, which is the beginning of the erosion process. Once the soil becomes fine particles, it rolls with the flow; some will be left on the ground while the other part will enter the river and be carried by the flow to become sediment transport. The soil particles' shape, size,

and weight will determine the amount and magnitude of sediment transport.

Table 2. Sediment Transport Formulas

Name:	Formula
Cadwell:	$Q_s=1.200 \times P1^{0.8}$
Savage:	$Q_s=0.219 \times P1$
Ijima, Sato, Aono, Ihii:	$Q_s=0.130 \times P1^{0.54}$
Ichikawa, Aichiai, Tomita, Murobuse:	$Q_s=0.130 \times P1^{0.8}$
Ijima, Sato:	$Q_s=0.060 \times P1$
Tanaka:	$Q_s=0.120 \times P1$
Komar, Inman:	$Q_s=0.778 \times P1$
Das:	$Q_s=0.325 \times P1$
CERC:	$Q_s=0.401 \times P1$

The Ijima Sato method was validated by comparing the similarity of coastline change patterns over 20 years calculated using sediment transport calculation methods in Table 1 with the coastline change maps available on Google Earth. The initial validation step involved creating an initial coastline using CAD by redrawing the current coastline from Google Earth. From this, we obtained the initial condition of the coastline. Subsequently, we identified the coastline from 20 years ago using Google Earth Pro and bathymetry maps to assess the actual coastline changes over the 20 years.

The next step involves comparing the predicted coastline change results over 20 years using sediment transport methods listed in Table 1. The calculation results are plotted on a bathymetry map to determine which method closely matches the

coastline changes observed in Google Earth. The coastline change calculations using the Ijima Sato method are then used to predict the erosion and sedimentation rates expected over the next 20 years before and after installing coastal protection structures such as groins. Similar techniques have been employed by (Paul et al., 2022). Their study analyzes the trend of coastal erosion in the Digha Coastal tract due to coastal protection structures.

RESULTS AND DISCUSSION

Administratively, the location of the study area is in the coastal area of Randuputih village (Figure 5), 1.5 kilometers long, which is located in the following administrative area Regency Probolinggo, East Java Province with astronomical limits as follows: 113°19'55.65” East longitude 7°45'19.54” South Latitude. Figure 6 is a bathymetric map of the coastal area in Probolinggo. This map was obtained from the Dinas Hidro Oseanografi TNI-AL (DISHIDROS). Bathymetric maps are used to model coastline changes.



Figure 5. Waves in the Randuputih Region

sedimentation containment efficiency level observed over 20 years. The calculation results and drawings in Figures 7 and 8 scheme are as follows:

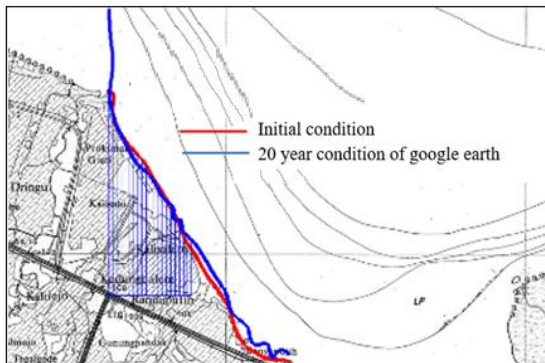


Figure 8. Changes in Coastline Initial Conditions and Conditions with Google Earth

Validation of Coastline Changes Over 20 Years

After modeling changes in coastlines, it is necessary to validate the modeling results using bathymetric maps and Google Earth maps (Figure 9-10). This is done to ensure the accuracy of the results.

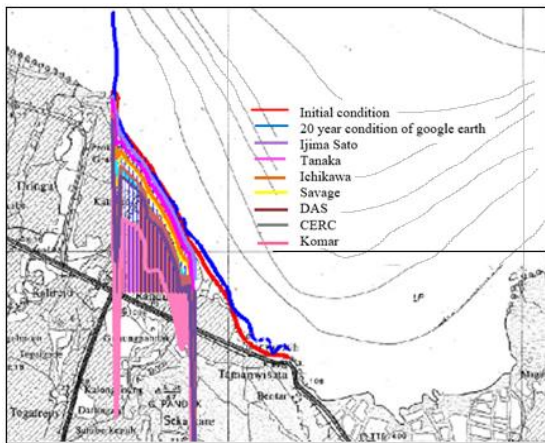


Figure 9. Changing Conditions of Coastlines Using Sediment Transport Methods

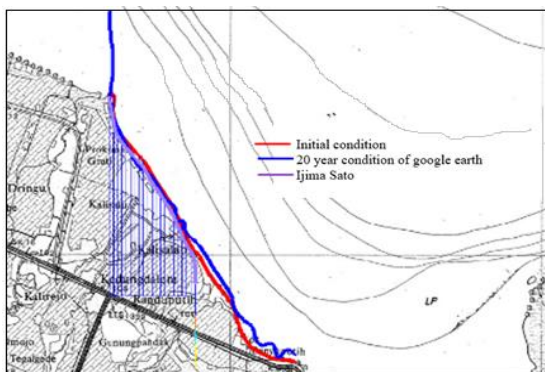


Figure 10. Condition of Initial Coastline Changes, Current Coastline Changes, and Coastline Changes Using the Ijima Sato Sediment Transport Method Approaching Coastline.

In figures 9-10, it can be seen that the Ijima Sato theory closely approximates the coastline change patterns during the initial condition and over 20 years on Google Earth. Detailed calculation results can be seen in Table 3.

Table 3. Coastline change over 20 years

Pias	Coastline initial condition (m)	Qs (m ³ /day)	Coastline over 20 years (m)	Percentage of change
0	2503.49	3.05	2127.83	-15.01%
1	2482.28	3.80	2014.93	-18.83%
2	2058.63	3.60	1616.25	-21.49%
3	1976.66	2.63	1652.81	-16.38%
4	1908.37	4.15	1397.44	-26.77%
5	1843.83	5.21	1203.13	-34.75%
6	1784.07	4.83	1190.18	-33.29%
7	1727.36	5.14	1095.26	-36.59%
8	1667.57	5.45	997.25	-40.20%
9	1594.77	3.12	1211.05	-24.06%
10	1495.22	3.75	1034.02	-30.84%
11	1408.50	3.60	966.12	-31.41%
12	1333.31	2.63	1009.45	-24.29%
13	1255.86	4.15	744.93	-40.68%
14	1171.23	2.20	900.66	-23.10%
15	1079.89	4.83	486.00	-55.00%
16	977.49	3.05	601.83	-38.43%
17	857.46	3.76	395.53	-53.87%
18	728.63	3.60	286.25	-60.71%
19	633.01	2.63	309.15	-51.16%
20	563.00	3.99	301.20	-46.50%

Table 3 presents the calculation results of coastline changes over 20 years using the Ijima Sato method. These calculation results are plotted in Figure 10. The calculations divide the coastline length into 21 pias (pias 1 to 20). Generally, the coastline experiences significant retreat is ranging from -15.01% to -60.71%. The average coastline retreat is -34%. The pias with the most considerable retreat is Pias 18, which experienced a coastline retreat of 60.71%, with an average sediment transport $Q_s = 3.74 \text{ m}^3/\text{day}$.

Modeling of Coastline Changes with Groins Design

Based on the calculations in Table 3, it is estimated that over the next 20 years, Randuputih Beach faces a high erosion risk, necessitating coastal protection measures. Groin-type coastal protection structures will be implemented, requiring modeling to assess their significant impact on coastline changes over

20 years. The groins will be installed along a long 700m. each with a crest width of 0.87m. totaling three groins spaced 350m apart. Figure 11 shows the groins' layout at Pias 3, 10, and 17.

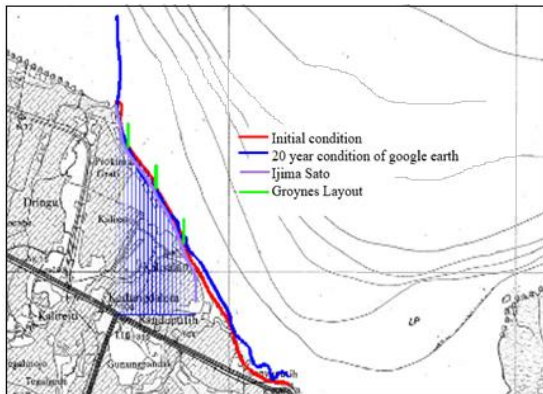


Figure 11. Modeling coastline with groins design

Validation of Comparative Analysis of Coastline Change Models

The coastline changes can be compared from the analysis and calculations. and the comparison graph can be seen in the image below. The graph in Figure 9-10 shows changes in the coastline over 20 years. and there has been quite a significant decline. The results of modeling coastline changes. considering sediment transport. also show changes. The results are quite accurate based on the calculation results that have been validated concerning bathymetric maps and Google Earth.

By considering the relationship between coastline changes and the Ijima Sato sediment transport. the forecast for coastline decline in the next 20 years after the construction of the groins is carried out is as follows (Figure 12):

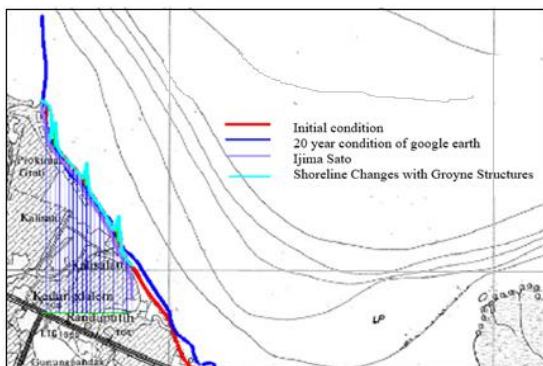


Figure 12. Conditions of Initial Coastline Changes, Current Coastline Changes, Coastline Changes Using the Ijima Sato Sediment Transport Method, and Coastline Changes with Groin Structures.

The Table 4 above shows coastline changes over 20 years after adding groin structures calculated using the Ijima Sato method. This data includes the initial

coastline. the coastline after 20 years with groins. and the percentage of coastline change. Installing three groins along 700m. each with a crest width of 0.87m and spaced 350m apart at Pias 3, 10, and 17. significantly influences coastline changes. Adding groin structures mitigates coastline retreat somewhat compared to the percentage change before groin installation (Table 3). This indicates

Table 4. Coastline changes after groin construction

Pias	Coastline initial condition (m)	Coastline changes over 20 years after groin construction (m)	Percentage of change
0	2503.44	2451.46	-2.12%
1	2482.24	2171.20	-14.33%
2	2058.59	2435.91	15.49%
3	2706.58	2706.58	0.00%
4	1908.34	1828.22	-4.38%
5	1843.80	1766.78	-4.36%
6	1784.03	1709.00	-4.39%
7	1727.33	1650.29	-4.67%
8	1667.54	1582.06	-5.40%
9	1594.74	1961.09	18.68%
10	2225.15	2225.15	0.00%
11	1408.47	1321.45	-6.59%
12	1333.29	1244.79	-7.11%
13	1255.84	1162.68	-8.01%
14	1171.21	1073.70	-9.08%
15	1079.87	975.19	-10.73%
16	977.47	1331.02	26.56%
17	1587.40	1587.40	0.00%
18	728.62	628.34	-15.96%
19	633.00	549.33	-15.23%
20	562.99	468.90	-20.07%

that groin structures can enhance coastline stability over 20 years. However. groin construction causes sedimentation and erosion in the surrounding areas. An example is around the groin at Pias 17. where significant sedimentation of 26.56% occurs (at Pias 16) and erosion at Pias 18. Similar conditions occur at the groins installed at Pias 3 and 10. This is also experienced in previous studies with similar coastal conditions and protective structures conducted in Camplong Beach, Madura (Purnawanti et al., 2020) and Eretan Beach, Indramayu (Hidayat, 2023). Adding groin structures can maintain coastline stability. but optimization is needed to reduce sedimentation and erosion around groin structures.

CONCLUSION

The construction of the groin caused increased sedimentation in areas initially experiencing erosion. The distribution of sediment transport over the width of the surf zone cannot be known. However, compared to other methods, the Ijima Sato method is a coastline change close to the coastline change in the Randuputih Probolinggo area with an average sediment transport of 3.74m^3 /day originating from the northwest direction. Through this study, a model of coastline changes due to erosion and sedimentation before

and after is studied concerning sediment transport using the Ijima Sato method. Breaking waves and several horizontal and vertical currents near the beach transport sediment along the coast. The installation of groins along 700 meters with three units and a crest width of 0.87 meters at Piass 3, 10, and 17 have significantly impacted coastline changes over 20 years. The average coastline retreat before the groins were built was 34%, whereas after the groins were built, the coastline retreat reached 6.61%.

REFERENCES

- Carvalho, B. C., & Guerra, J. V. (2024). Estimates of longshore sediment transport rates along Macumba and Recreio-Barra da Tijuca sandy beaches (Rio de Janeiro) southeastern. *International Journal of Sediment Research*, 39(3), 317–326. <https://doi.org/10.1016/j.ijsrc.2024.03.005>
- Donatus, B., Adade, R., Obeng, E., Dzantor, S., Kwadzo, E., & Agbeko, P. (2023). Heliyon Effects of coastal protection structures in controlling erosion and livelihoods. 9 (October).
- Fellowes, T. E., Vila-Concejo, A., Gallop, S. L., Schosberg, R., de Staercke, V., & Largier, J. L. (2021). Decadal coastline erosion and recovery of beaches in modified and natural estuaries. *Geomorphology*, 390, 107884. <https://doi.org/10.1016/j.geomorph.2021.107884>
- Fernandes, D., & Castro, A. (2024). *Journal of South American Earth Sciences* Longshore sediment transport rate in Formosa Bay, Rio de Janeiro State - Southeast Brazil. 137 (September, 2023). <https://doi.org/10.1016/j.jsames.2024.104834>
- Gurgel Vasconcelos, Y., Pereira de Paula, D., Manuel Ferreira, Ó., & Leisner, M. M. (2024). Contrasting short-term coastline behavior after the construction of sinusoidal groins in NE Brazil. *Journal of South American Earth Sciences*, 136(February). <https://doi.org/10.1016/j.jsames.2024.104832>
- Hanes, D. M. (2022). 8.04 - Longshore Currents. In J. (Jack) F. Shroder (Ed.), *Treatise on Geomorphology (Second Edition) (Second Edition)*, pp. 83–99. Academic Press. <https://doi.org/https://doi.org/10.1016/B978-0-12-818234-5.00051-1>
- Hidayat, G. S. (2023). Perencanaan tata letak groin untuk menanggulangi abrasi dan erosi di pantai eretan indramayu. 68–76.
- Kumaseh, E., Tatontos, Y. V., & Sarapil, C. I. (2020). Prediksi Transport Sedimen di Perairan Teluk Tahuna Kabupaten Kepulauan Sangihe. *Journal of Marine Research*, 9(3), 207–214. <https://doi.org/10.14710/jmr.v9i3.26537>
- Manno, G., Lo Re, C., Basile, M., & Ciraolo, G. (2022). A new coastline change assessment approach for erosion management strategies. *Ocean and Coastal Management*, 225(July 2021), 106226. <https://doi.org/10.1016/j.ocecoaman.2022.106226>
- Marghany, M. (2021). Chapter 8 - Polarimetric synthetic aperture radar for wave spectra refraction using inversion SAR wave spectra model. In M. Marghany (Ed.), *Nonlinear Ocean Dynamics* (pp. 215–246). Elsevier. <https://doi.org/https://doi.org/10.1016/B978-0-12-820785-7.00008-3>
- Paul, S., Chowdhury, S., & Chaudhuri, S. (2022). Analyzing the trend of beach–dune erosion in the Digha coastal tract in response to nearshore wave processes and coastal protection structures. 52.
- Pratama, M. I., Legono, D., & Rahardjo, A. P. (2019). Analisis Transpor Sedimen Serta Pengaruh Aktivitas Penambangan Pada Sungai Sombe, Kota Palu, Sulawesi Tengah. *Jurnal Teknik Pengairan*, 10(2), 84–96. <https://doi.org/10.21776/ub.pengairan.2019.010.02.02>
- Purba, J. R. N. D., Setiyono, H., Atmodjo, W., Muslim, M., & Widada, S. (2022). Pengaruh Kondisi Oseanografi Terhadap

- Pola Sebaran Sedimen Dasar di Perairan Mangunharjo.
Kota Semarang. Indonesian Journal of Oceanography. 4(1). 77–87.
<https://doi.org/10.14710/ijoce.v4i1.13214>
- Purnawanti. Y. N., Ayunda. L. D., & Santoso. A. R. (2020). Studi Perencanaan Revetment dan Groin Sebagai Upaya Penanganan Erosi Pantai Camplong di Kabupaten Sampang Madura. Jurnal Teknik Transportasi. 1(1). 70.
<https://doi.org/10.54324/jtt.v1i1.431>
- Trombetta. T. B. (2020). An overview of longshore sediment transport on the Brazilian coast ☆. Regional Studies in Marine Science. 35. 101099.
<https://doi.org/10.1016/j.rsma.2020.101099>
- Triatmodjo. B. (1999). Teknik Pantai. Beta Offset.
- Umar. H., Rachman. T., & Alkhaer. I. (2023). Analisis Longshore Current Dan Longshore Sediment Transport Pada Pantai Aeng. Galesong Utara. Kabupaten Takalar. Jurnal Ilmu Dan Teknologi Kelautan Tropis. 15(3). 327–340.
<https://doi.org/10.29244/jitkt.v15i3.43159>